Am J Physiol Renal Physiol 308: F938–F949, 2015.
First published February 5, 2015; doi:10.1152/ajprenal.00655.2014.

Mechanism by which shock wave lithotripsy can promote formation of human calcium phosphate stones

Andrew P. Evan,[1,2] Fredric L. Coe,[3] Bret A. Connors,[1] Rajash K. Handa,[1] James E. Lingeman,[2] and Elaine M. Worcester[3]

[1]*Department of Anatomy and Cell Biology, Indiana University School of Medicine, Indianapolis, Indiana;* [2]*International Kidney Stone Institute, Methodist Hospital, Indianapolis, Indiana; and* [3]*Nephrology Section, University of Chicago, Chicago, Illinois*

Submitted 17 December 2014; accepted in final form 29 January 2015

Evan AP, Coe FL, Connors BA, Handa RK, Lingeman JE, Worcester EM. Mechanism by which shock wave lithotripsy can promote formation of human calcium phosphate stones. *Am J Physiol Renal Physiol* 308: F938–F949, 2015. First published February 5, 2015; doi:10.1152/ajprenal.00655.2014.—Human stone calcium phosphate (CaP) content correlates with higher urine CaP supersaturation (SS) and urine pH as well as with the number of shock wave lithotripsy (SWL) treatments. SWL does damage medullary collecting ducts and vasa recta, sites for urine pH regulation. We tested the hypothesis that SWL raises urine pH and therefore Cap SS, resulting in CaP nucleation and tubular plugging. The left kidney (T) of nine farm pigs was treated with SWL, and metabolic studies were performed using bilateral ureteral catheters for up to 70 days post-SWL. Some animals were given an NH_4Cl load to sort out effects on urine pH of CD injury vs. increased HCO_3^- delivery. Histopathological studies were performed at the end of the functional studies. The mean pH of the T kidneys exceeded that of the control (C) kidneys by 0.18 units in 14 experiments on 9 pigs. Increased HCO_3^- delivery to CD is at least partly responsible for the pH difference because NH_4Cl acidosis abolished it. The T kidneys excreted more Na, K, HCO_3^-, water, Ca, Mg, and Cl than C kidneys. A single nephron site that could produce losses of all of these is the thick ascending limb. Extensive injury was noted in medullary thick ascending limbs and collecting ducts. Linear bands showing nephron loss and fibrosis were found in the cortex and extended into the medulla. Thus SWL produces tubule cell injury easily observed histopathologically that leads to functional disturbances across a wide range of electrolyte metabolism including higher than control urine pH.

histopathology; pH regulation; renal function; thick ascending limb

IDIOPATHIC CALCIUM PHOSPHATE (CaP) stone formers (IPSF) differ from the more common idiopathic calcium oxalate (CaOx) stone formers (ICSF) in forming not only kidney stones but also hydroxyapatite (HA) plugs in their ducts of Bellini (BD) and inner medullary collecting ducts (IMCD) with consequent papillary inflammation, retraction, and epithelial cell loss (8–10). Whereas the renal cortices of ICSF are normal, those of IPSF show focal scarring (9, 10).

CaP stones, especially those composed of brushite (BR; calcium monohydrogen phosphate), are difficult to treat urologically (6, 13, 14, 17, 29). HA and BR stones tend to be large, often forming a staghorn configuration. Their size can preclude management with shock wave lithotripsy (SWL) or ureteroscopy (URS). Because BR stones are resistant to SWL, and large, 75% of patients in a recent study required percutaneous nephrolithotomy (PNL) (14). CaP stones rapidly recur (14), and nephrocalcinosis is common (1).

Urine CaP supersaturation (SS), which drives CaP crystallization, rises with pH in the range between 6 and 6.5 (29). As expected, human stone CaP content correlates with higher urine CaP SS and urine pH (29). Another correlate of stone CaP content is the number of SWL treatments a patient has received (29); no apparent reason for this association has hitherto been adduced.

Patients can convert from ICSF to IPSF, and those that convert have higher urine pH when forming CaOx stones than do those ICSF who do not convert (27). SWL procedures were more frequent among those ICSF who converted to IPSF (26). Stone CaP% has increased in the past three decades (4, 20, 21, 24, 29), which coincides with the introduction of SWL for stone treatment (5, 18).

One possible explanation for the increase in stone CaP% over time, and for statistical links between SWL and both stone CaP% and conversion from ICSF to IPSF, is that SWL raises urine pH and therefore CaP SS. Even if only transient, higher SS could engender CaP nucleation and tubule plugging. Papillary injury might then raise tubule fluid pH with further CaP formation.

Final urine pH is achieved in the collecting ducts (CD) via proton transport by intercalated cell vacuolar-type H^+-ATPase (V-ATPase). The shock wave field from even narrowly focused instruments affects most of a human papillum and medulla because of respiratory motion (11). The primary injury is vascular disruption (7, 36) with hemorrhage and interstitial blood pooling. Cavitation within interstitial blood pools damages epithelial cells (23, 25). Outer and inner medullary collecting ducts (OMCD and IMCD), and medullary thick ascending limbs (mTAL) are at obvious immediate risk of injury, similarly for medullary (S3) proximal tubule (PT) segments.

Cells in the mTAL are especially vulnerable to long-term ischemic injury from SWL. Their "arterial" blood supply arises partly from thin-walled ascending vasa recta (16) which lie within the shock field of SWL focused on papillary stones, and would be the first line of vessels to be injured (11). Therefore, mTAL cells incur both acute injury from local cavitation and longer term ischemia as vasa recta in the inner medulla reorganize.

SWL injury of OMCD and possibly cortical CD (CCD) could compromise H^+ transport, raising tubule fluid and local calyceal pH. Alternatively, since mTAL reabsorb bicarbonate (2), SWL damage could increase bicarbonate delivery to OMCD, raising tubule fluid and urine pH even if the V-ATPase

Address for reprint requests and other correspondence: E. M. Worcester, Univ. of Chicago Medicine, Nephrology Section/MC5100, 5841 South Maryland Ave., Chicago, IL 60637 (e-mail: eworcest@uchicago.edu).

were normal. In addition to mTAL, cortical TAL (cTAL) and even PT might increase bicarbonate delivery to OMCD. The untreated kidney will maintain blood HCO_3^- concentration at a normal level that perpetuates high distal HCO_3^- delivery in the SWL-treated kidney.

We have tested the SWL pH hypothesis using pigs with bilateral ureteral catheters, which permits comparison of urine pH between SWL-treated and control kidneys. To sort out effects on urine pH of CD injury vs. increased HCO_3^- delivery, we reduced serum HCO_3^- and therefore HCO_3 delivery via NH_4Cl loading. We also measured a variety of transported solutes to distinguish between TAL and PT as sources of increased CD bicarbonate delivery.

If correct, the SWL pH hypothesis could affect how kidney stones are managed. Because CaP stones are harder to treat and produce more tissue injury than CaOx stones, treatment modalities such as URS with laser lithotripsy (17) may become favored over SWL with eventual changes in practice guidelines and urological practice.

METHODS

Animals and Design

Animals. Nine female Gottingen pigs (12–32 kg on arrival, Marshall BioResources, North Rose, NY) were studied (Table 1) in 14 experiments (animal care review approval no. 3059). Pigs ate standard chow (Laboratory Porcine Grower Diet, no. 5084, LabDiet, St. Louis, MO) for 1 wk before SWL of 1 kidney. All but one pig (*pig 983*) were aged 45–58 wk at the end of the study; the exception was 27 wk.

Design of study. Our principal hypothesis is that SWL raises urine pH. To test this, we treated one kidney of each animal with SWL, waited for varying numbers of weeks thereafter (Table 1), inserted bilateral ureteral catheters, and compared the difference in urine pH between treated (T) and control (C) kidneys (T − C) against 0.

Since a difference in pH, if present, might arise from injury to CD cells, increased HCO_3^- delivery to CD, or both, we administered ammonium chloride (NH_4Cl) in 10 of our 14 experiments (all 9 pigs received NH_4Cl). A pH difference caused simply by increased HCO_3^- delivery would be abolished. One due to cell injury would not.

Baseline comparison measurements were not made before SWL because this protocol involves multiple animal survival surgeries, and baseline measurements would have added an additional survival surgery, which would have reduced the numbers of the more critical post-SWL studies. Intervals following SWL are not exactly the same for every animal because of practical considerations such as availability of facilities, surgeons, and personnel, and full health of the animal after the prior surgery.

Animals were euthanized with an iv injection of barbituric acid derivative at 100–150 mg/kg body weight. Both kidneys were harvested (Table 1) for detailed study.

Table 1. *Summary of pigs and experiments*

Pig	Experiment	Days	No. of Periods	
			Basal	Acid load
910	1	28	9 (8)	
910	2*	56	4 (4)	8 (8)
912	1	34	2 (0)	
912	2*	47	4 (4)	6 (5)
916	1	28	2 (2)	9 (8)
916	2*	60	4 (4)	14 (14)
921	1	39	4 (4)	
921	2	56	5 (0)	7 (0)
921	3*	67	5 (4)	
983	1*	36	5 (5)	4 (4)
1037	1*	29	4 (4)	6 (4)
1038	1*	70	5 (4)	4 (3)
1039	1*	70	4 (4)	7 (7)
1040	1*	70	4 (4)	8 (8)
Totals			61 (51)	73 (61)

*Experiment after which pig was euthanized; days, days between SWL and experiment. No. of periods, periods during which urine was collected (periods with matching blood sample).

Surgical Procedure

Anesthesia, instrumentation, and SWL. Anesthesia, hydration, monitoring, catheter placement (Open End Ureteral Catheters, Boston Scientific, Natick, MA), and SWL were as in our other studies (35). However, animals were conserved after SWL for the experiments already mentioned. All animals received 1% of body weight per hour as normal saline.

Experimental Procedure

Sample collections. Two to nine baseline urine and blood samples were collected from each kidney at 30-min intervals during each experiment (Table 1). On at least one occasion, each pig then received NH_4Cl, and 4–14 additional blood and urine samples were collected at 30-min intervals. All urine samples were collected under mineral oil to avoid changes in pH due to atmospheric CO_2. A paired blood sample was obtained with each urine.

Acid loading. Over 1–2 min, 3.7 meq NH_4Cl/kg body weight was delivered iv (venous HCO_3^- 27 ± 0.4 vs. 18.2 ± 0.4, basal and post NH_4Cl, respectively; $P < 0.05$).

Kidney preservation and harvesting. After completion of the terminal experiment for each animal (Table 1, asterisk), kidneys were perfusion fixed with 10% phosphate-buffered formalin using a previously described procedure (31).

SWL Technique

SWL was carried out as described in our other publications (used unmodified Dornier HM3) (35). Four individual 2,000 SW treatments (24 kV and 120 SWs/min) were delivered so that the entire kidney from lower to upper pole was covered during one treatment session with a total of 8,000 SWs.

Urine Measurements

pH. Urine pH was determined within 15 min using a Mettler Toledo SevenMulti pH meter (Mettler Toledo, Schwerzenbach, Switzerland) with an Orion Ross Semi-Micro Sure-Flow pH electrode (Thermo Scientific, Waltham, MA).

Other analytes. Urine and serum sodium, potassium, total HCO_3^-, creatinine, Ca, Mg, Cl, phosphate, and urate, as well as urine NH_4, SO_4, and lithium were measured as previously described (28, 37).

Histological Techniques

All treated kidneys except from *pig 912* were divided into four cross-sectional zones: lower pole, lower midpole, upper midpole, and upper pole. Control kidneys were divided into their lower and upper zones. These were routinely processed and stained with either hematoxylin/eosin, or picro-sirus red for defining fibrotic areas (31).

To count the number of fibrotic bands in each zone, a section from each zone was placed on a light box and the number of fibrotic bands was counted across the entire cortical region of the section. These same sections were then examined under a microscope to determine the number of papilla present in each section and how many showed evidence of injury. The stained sections were examined with a Leica DME microscope (Leica Microsystems, Deerfield, IL) mounted with a Spot Slider digital camera (Spot Imaging Solutions, Sterling Heights, MI).

The outer diameters of 50 mTAL and OMCD seen in cross section from injured papilla of eight animals were measured using a micrometer insert that was placed in the eyepiece of a light microscope. Tissues were measured using a ×40 objective. At the same time, the number of visible nuclei was counted in each of the 50 cross sections of mTAL and OMCD.

Immunohistochemical Localization of Ki-67 Protein

Separate sections were processed for immune localization of Ki-67 protein to detect proliferating cells (30). Routine immunohistochemical techniques for the detection of Ki-67 (monoclonal antibody, Abcam, Cambridge, MA)-positive staining were performed as previously published (38). Controls were performed with the elimination of the primary antibody and showed no staining. Sections from *pigs 916*, *921*, and *983* were analyzed.

Calculations

Excretion rates and clearances were calculated conventionally. We compared excretion rates by taking the difference between the treated and control kidneys so as to have a comparator with the units of excretion rates.

To compare tubule function of the two kidneys, we compared fractional excretions (FE) for materials of interest. FE is the urine excretion divided by filtered load:

$$\mathrm{FE}[x] = (\mathrm{U}[x] * \mathrm{V})/(g * \mathrm{P}[x]) \quad (1)$$

where x is any material of interest, U[x] and P[x] are urine and plasma concentrations, or ultrafiltrate concentrations if protein bound, and g is glomerular filtration rate. Since g = U[m]*V/P[m] where m is a filtration marker like inulin or creatinine, Eq. 1 becomes:

$$\mathrm{FE}[x] = (\mathrm{U}/\mathrm{P})x/(\mathrm{U}/\mathrm{P})\mathrm{m}. \quad (2)$$

Our purpose is to compare the treated with the control kidney, which share a blood circulation and therefore identical values for plasma concentrations. Therefore the ratio of their FE is:

$$\mathrm{FE}[x]\mathrm{t}/\mathrm{FE}[x]\mathrm{c} = (\mathrm{U}x/\mathrm{Um})\mathrm{t}/(\mathrm{U}x/\mathrm{Um})\mathrm{c} \quad (3)$$

or simply the ratio of the urine concentration ratios for x over the filtration marker (m) in the treated (t) kidney divided by that for the control kidney (c).

We could have compared differences in FE values but chose the ratio for several reasons. FE is itself a unitless fraction, so differences would not preserve specific units. The ratio of FE values provides a unitless scale passing through 1 at identity and offering a simple quantification above and below 1; the ratio cancels out plasma values. We lacked serum oxalate and lithium measurements, but could nevertheless calculate FE ratio values for both.

We lacked serum creatinine values for 22/134 clearance periods (Table 1). For 51 control and 61 NH_4Cl periods, we had complete data and calculated the significance of the CCr difference between T and C kidneys (Tables 2 and 3) using paired *t*-tests and ANOVA. Since creatinine clearance is Ucr*V/Pcr, the difference in clearance T − C is [Ucr(t) − Ucr(c)]*1/Pcr. Since 1/Pcr is simply a scaling term that does not affect statistical testing, we tested the creatinine excretion difference against 0 using paired *t*-tests and in ANOVA models, for the total of 61 basal and 73 NH_4Cl periods. As we found no significant difference for either the limited set of complete data, or the larger set using only urine values, we show the data only for the complete cases in Tables 2 and 3. Since we could calculate the ratio of CCr without serum creatinine values, we present this ratio in our figures. Our FE ratio calculations for specific analytes (Tables 2 and 3) do not require serum creatinine (Eq. 3) and so are not limited by the missing values.

We lacked urine and serum osmolality measurements but could calculate electrolyte-free water clearance:

Table 2. *Paired t-test means for excretion differences between treated (T) and control (C) kidneys*

	No. of Observations		T − C Excretion Difference	
Urine Values	Basal	Acid load	Basal	Acid load
pH	61	73	**0.18 [0.09, 0.27]**	−0.03 [−0.08, 0.02]
HCO_3^-, μmol/min	54	67	**15 [3.6, 26.4]**	4.2 [−0.2, 8.6]
Flow, ml/min	61	73	**0.55 [0.38, 0.72]**	**0.17 [0.05, 0.28]**
K, μeq/min	61	73	**16.9 [12.2, 21.6]**	−0.96 [−5.4, 3.5]
Cl, μeq/min	61	73	**67.2 [45.8, 88.6]**	13.3 [−3.6, 30.2]
Sulfate, μeq/min	61	71	**3 [1.7, 4.3]**	0.31 [−0.4, 1]
Ca, μg/min	60	72	**25.2 [13.5, 37]**	−3.5 [−9.9, 3.0]
Mg, μg/min	61	73	**28.4 [15.5, 41.6]**	4.1 [−1.5, 9.6]
Na, μeq/min	61	73	**66.3 [42.3, 90.3]**	13 [−0.94, 26.8]
Phosphate, μg/min	56	73	**0.5 [−2.6, 3.7]**	**−2.1 [−3.5, −0.8]**
Oxalate, μg/min	43	44	**2.7 [1.1, 4.2]**	−0.66 [−2.4, 1.1]
Urate, μg/min	43	46	0.1[−0.3, 0.5]	−0.3[−0.7, 0.1]
CCr, ml/min	51	61	1.3 [−1.2, 3.8]	−1.2 [−2.9, 0.46]
NH_4, μmol/min	61	73	0.12 [−1.2, 1.5]	0.6 [−1.6, 2.8]

Values are means with 95% confidence interval (CI; []). CCr, creatinine clearance. Bold, differs from 0, $P < 0.05$.

$$\mathrm{CH_2O} = \mathrm{V} * (1 - (\mathrm{U}[\mathrm{Na}] + \mathrm{U}[\mathrm{K}])/(\mathrm{P}[\mathrm{Na}])) \quad (4)$$

Statistical Analysis

Differences in excretion rate and ratios of FE of basal and NH_4Cl-loading conditions were compared by paired *t*-tests, and using ANOVA with time from SWL as a covariate. Excretion rate differences and FE ratios within the ANOVA model were compared with 0 and 1, respectively, to assess significance of deviations between the kidneys. Calculations were done using Systat (San Jose, CA).

RESULTS

As expected, C kidneys were not abnormal, having received no ESWL treatment. Therefore, they are not referred to except when specific quantitative differences from T kidneys are presented. Because Tables 1–3 were introduced in METHODS, the RESULTS begin with Table 4.

General Renal Injury in T Kidneys

On both kidney surfaces and from the upper to lower pole, fibrotic bands (arrows) extended from the renal capsule to the renal papillum (Fig. 1, *A* and *B*; Table 4) and created dimpling at the renal capsule (double arrows). The majority of papillae were injured in T kidneys (Table 4). Whereas cortical injury was focal, papillary injury was either absent or generalized; in other words, when papillae were injured the injury was diffuse across the entire papillum.

Segmental Nephron Injury in T Kidneys

Cortical segments. The vast majority of cortex was normal, as bands were sparse and nephron structures not in or adjacent to bands were normal. Within bands, nephrons were obliterated (Fig. 2, *A–E*). PT adjacent to fibrotic bands (Fig. 2, *C–F*) varied from normal to abnormal with thickening of basement membranes (arrows), reduced overall diameter, smaller epithelial cells, and even complete obliteration (asterisks). Adjacent glomeruli varied from normal to sclerotic (Fig. 2, *B* and *D*). Adjacent CCD and cTAL varied from normal to dilated and elongated (Fig. 2, *C* and *D*), but their cells always appeared normal.

Table 3. *ANOVA of T − C differences from 0 and T/C fractional excretion ratio from 1*

	T − C Excretion Difference		T/C FE Ratio	
Urine Values	Basal	Acid load	Basal	Acid load
Arterial pH	**0.13 ± 0.04**	−0.04 ± 0.04*		
Adjusted pH	**0.17 ± 0.04**	−0.03 ± 0.03*		
HCO_3^-, μmol/min	**15 ± 4**	4 ± 4	**3 ± 0.9**	1.5 ± 0.8
Flow, ml/min	**0.5 ± 0.07**	**0.18 ± 0.07***#	—	
K, μeq/min	**16 ± 2**	−0.3 ± 2*#		
Cl, μeq/min	**65 ± 10**	15 ± 9*#	**3.3 ± 0.7**	2.2 ± 0.6#
Sulfate, μeq/min	**2.9 ± 0.5**	0.4 ± 0.5*#	**1.7 ± 0.2**	**1.3 ± 0.1**#
Ca, μg/min	**25 ± 5**	−3 ± 4*	**3.1 ± 0.6**	2 ± 0.6#
Mg, μg/min	**28 ± 5**	4 ± 4*	**2.2 ± 0.2**	**1.4 ± 0.2**#*
Na, μeq/min	**65 ± 10**	14 ± 9*	**5 ± 2**	3 ± 1#
Phosphate, μg/min	0.6 ± 1	**−2 ± 1**	1.15 ± 0.09	0.99 ± 0.08
Oxalate, μg/min	**2.5 ± 0.8**	−0.44 ± 0.8*#	**1.14 ± 0.06**	1.11 ± 0.06
Urate, μg/min	0.1 ± 0.2	**−0.3 ± 0.2**	**1.3 ± 0.1**	1 ± 0.1
CCr, ml/min	1 ± 1	−1 ± 1		
NH_4, μmol/min	0.04 ± 1	0.7 ± 0.9		
FE lithium			**1.454 ± 0.167**	1.187 ± 0.129
CH_2O, ml/min	−0.036 ± 0.024	**0.075 ± 0.023***		
[Na+K], mmol/l	**7 ± 3**	−4 ± 3*		
Urea, μmol/min	**12 ± 3**	2 ± 3*		
Urea, mmol/l	**−29 ± 4**	**−19 ± 4**		

Values are ANOVA means ± SE for basal and acid load (NH_4Cl) conditions adjusted for days since shock wave lithotripsy (SWL) treatment except arterial pH, which is adjusted for arterial pH measured before and during the acid load. FE, fractional excretion; CH_2O, free water clearance. Bold, adjusted mean value ≠0 for differences, ≠1 for ratios. *Differs from basal, $P < 0.05$. #, Slope dependence on time from SWL, $P < 0.05$ (# is placed with acid load values but applies to both conditions in the ANOVA model).

Outer medulla. The outer medulla of injured papillae were diffusely abnormal. Structures in bands were obliterated (Fig. 1, *insets* in *A* and *B*; Fig. 3*A*). Outside of bands, almost all mTAL and OMCD showed wavy irregularity (Fig. 3, *A–E*). Lining cell epithelium of some OMCD was focally heaped up in a polypoid configuration, a definitive sign of hyperplasia (Fig. 3*E*). The S3 segments of PT (Fig. 3*F*) adjacent to bands showed the variable loss of cell height and basement membrane thickening observed in cortical PT; however, unlike OMCD and mTAL, most S3 appeared normal. Diffuse interstitial cellularity and fibrosis accompanied generalized OMCD and mTAL damage (Fig. 1, *insets* in *A* and *B*; Fig. 3, *A–F*).

Outer tubule diameters of, and numbers of cell nuclei in, OMCD and mTAL of T kidneys exceeded those in C (Table 5). Tubule diameters in T kidneys did not vary with time of harvest (compare Tables 1 and 5). These abnormalities affected most tubules.

As documented by nuclear staining for Ki-67, the higher number of cell nuclei in tubules of T vs. C kidneys reflected ongoing as opposed to prior proliferation (Fig. 4, *A* and *B*). For *pigs 916*, *921*, and 983, we found 6, 2, and 4 mTAL dividing cells per 100 tubule cross sections in C kidneys, vs. 324, 274, and 272, respectively, per 100 tubule cross sections in T kidneys. For OMCD, corresponding numbers were 6, 6, and 4 vs. 278, 288, and 258 (*P* values all <0.001). Counts in the

Table 4. *Injury in T and C kidneys*

		Fibrotic Bands					Papillary Injury				
Pig	Kidney	*Zone 1*	*Zone 2*	*Zone 3*	*Zone 4*	Mean	*Zone 1*	*Zone 2*	*Zone 3*	*Zone 4*	%Injured
910	C	1		1		1	0/2		1/3		20
	T	6	8	17	4	8.75	2/2	1/1	1/1	1/2	83
916	C	2		3		2.5	1/2		1/2		50
	T	15	10	10	9	11	4/4	2/2	2/2	3/3	100
921	C	3		3		3	1/4		0/2		17
	T	10	7	9	8	8.5	1/3	1/3	3/3	3/3	67
983	C	0		0		0	0/2		0/2		0
	T	0	6	9	10	6.25	1/2	1/1	2/3	2/2	75
1037	C	0		0		0	0/2		0/2		0
	T	6	4	7	6	5.75	1/2	2/2	3/3	2/2	89
1038	C	0		0		0	0/2		0/2		0
	T	1	3	5	0	2.25	0/2	0/3	1/2	0/2	11
1039	C	0		0		0	0/2		0/2		0
	T	8	9	6	4	6.75	2/2	1/2	1/2	1/3	55
1040	C	0		0		0	0/2		0/2		0
	T	5	7	2	2	4	2/2	2/2	1/2	1/3	67

Fibrotic bands, no./zone; papillary injury, no. injured papillae/total papillae in zone; *zone 1*, lower pole; *zone 2*, lower midpole; *zone 3*, upper midpole; *zone 4*, upper pole.

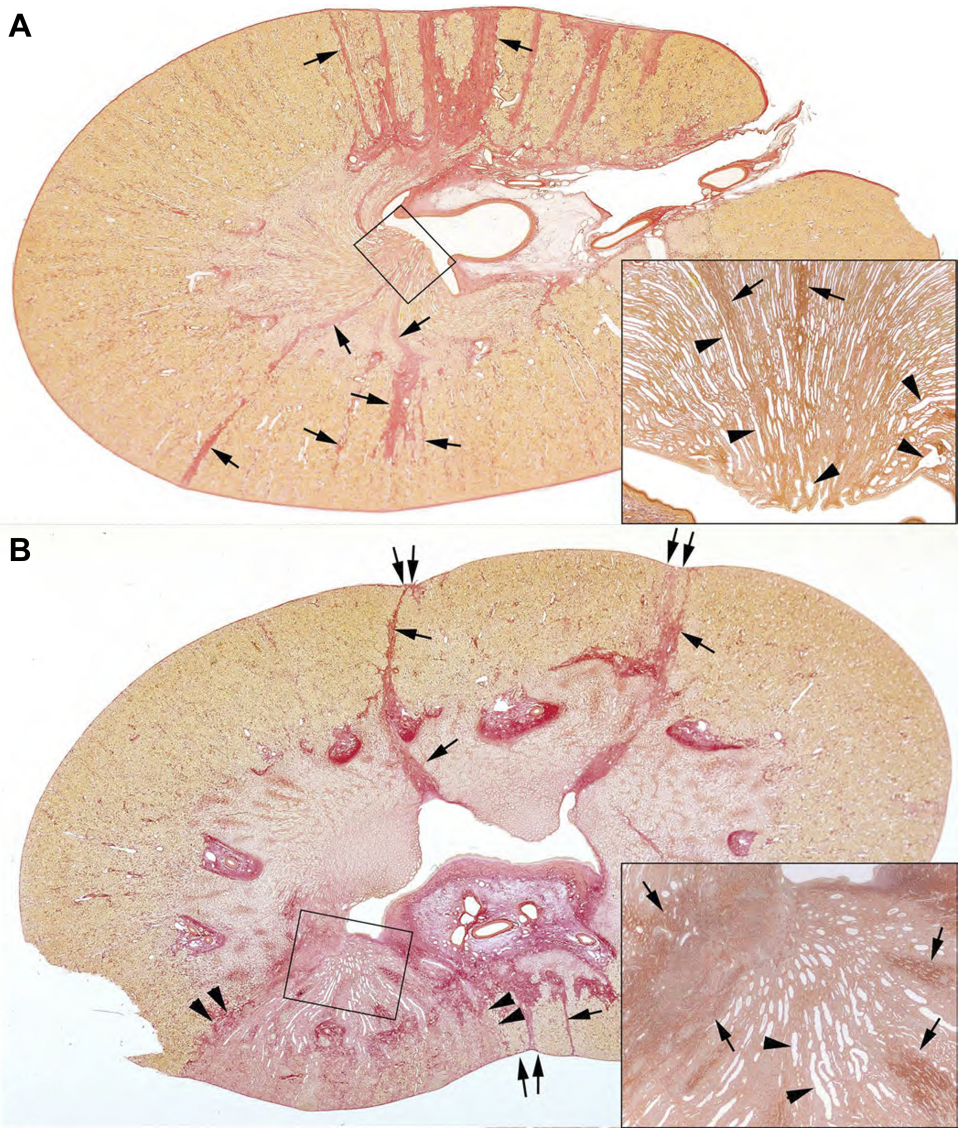

Fig. 1. Low-magnification light micrographs of *zone 3* of *pig 910* (*A*) and *zone 4* of *pig 921* (*B*) seen in transverse sections stained with picro-sirus red. Prominent reddish-stained bands are noted extending from the renal capsule as far down as the inner medulla (arrows), which define regions of interstitial fibrosis. Occasionally, these bands are associated with dimpling at the renal capsule (*B*, double arrows). In *B*, extensive scarring is noted to an entire renal lobule, which is outlined by a series of double arrowheads. A papillum from each section (outlined by a rectangle) is enlarged and seen as an *inset* at the *bottom right* of *A* and *B*. Bands of interstitial fibrosis are easily seen in the outer and inner medulla (arrows), which are interdispersed with dilated tubular profiles of inner medullary collecting ducts (single arrowheads).

36-wk kidneys (*pig 983*) did not differ from those of the 60- and 67-wk kidneys.[1]

Inner medulla and papillum. Like OMCD and mTAL, virtually all IMCD were variably elongated and thrown into a wavy irregularity (Fig. 1, *insets* in *A* and *B*). Thin loops were normal to completely atrophic. Because virtually all IMCD were injured, the interstitium was fibrotic (Fig. 1, *insets* in *A* and *B*).

Urine pH

Mean T − C difference. Whether unadjusted (Table 2), or adjusted for time since SWL or for arterial blood pH (Table 3), basal urine pH of T exceeded that of C. The individual T kidney urine pH values (Fig. 5, *top left*, *y*-axis) exceeded paired C values (*x*-axis) in a majority of instances, as judged by the position of points above the diagonal line of identity. NH_4Cl abolished the mean pH difference (Tables 2 and 3); individual pH values from T and C kidneys cluster around the line of identity (Fig. 5, *top right*). Further adjustments, for serum HCO_3^- or for difference in filtered load of HCO_3^-, did not affect the T − C urine pH difference (not shown). Without the paired design, the difference between the kidneys in the basal state is not statistically different.

pH changes with NH_4Cl. With acid loading, urine pH of the T kidney fell significantly (6.42 ± 0.09 vs. 6.12 ± 0.08, $P = 0.012$) whereas pH from the C kidney did not (6.24 ± 0.08 vs. 6.14 ± 0.08 $P = 0.36$). As judged by individual two- sample *t*-tests, reduction of urine pH was significant in 7/14 C and 6/14 T kidneys (not shown).

Serum HCO_3^- and filtered load of HCO_3^-. During the basal periods (Fig. 5, *bottom left*, gray circles), the urine pH difference (*y*-axis) did not vary with serum HCO_3^- (*x*-axis). After NH_4Cl, serum HCO_3^- was lower (black circles), and the linear regression was significant [coefficient = 0.017 (0.002, 0.031, 95% confidence interval), $P = 0.026$]. The basal T − C pH difference varied with the T − C filtered load of bicarbonate (Fig. 5, *bottom right*, gray circles) whereas after NH_4Cl (black

[1] We cannot find any other reports of mTAL cell proliferation in human kidneys. It was observed in a strain of Dahl salt-sensitive rats fed a high-NaCl diet (38).

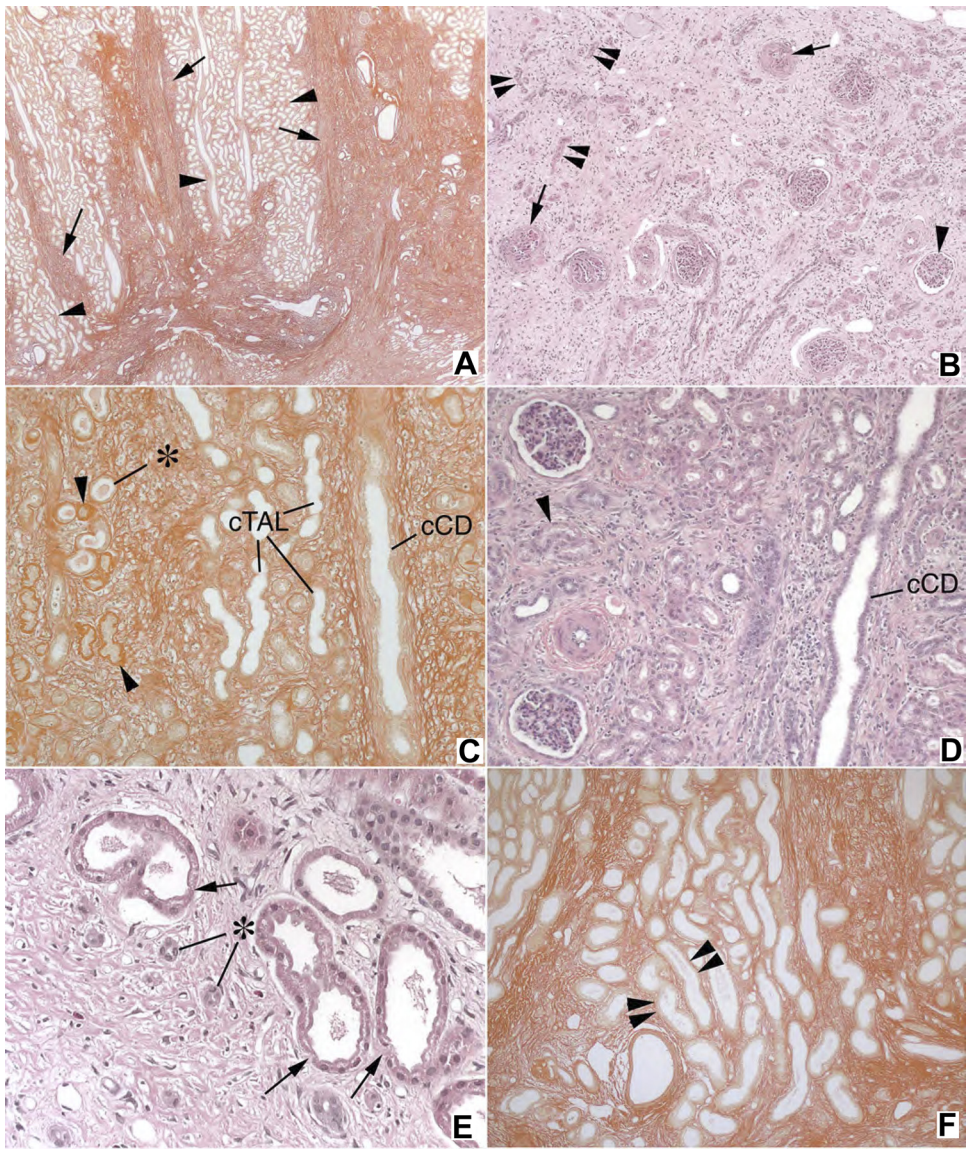

Fig. 2. Segmental nephron injury in the cortex of treated kidneys. *A*: sharp transition from regions of interstitial fibrosis (arrows) to normal-appearing nephron segments (arrowheads) in a picro-sirus red-stained section. *B*: within sites of interstitial fibrosis, glomeruli appear normal (arrowheads) to sclerotic (arrows), while many nearby tubular segments appear small and atrophic (double arrowheads). Cortical collecting ducts (CCD) and thick ascending limbs (cTAL) adjacent to regions of interstitial fibrosis appear dilated with normal-appearing cells (*C* and *D*). Proximal tubules adjacent to fibrotic bands varied from normal (*F*, double arrowheads) to thickening of basement membranes with reduced overall diameter (*C*, arrowheads), smaller epithelial cells (*E*, arrows), and even complete obliteration (*C* and *E*, asterisk).

circles), when serum HCO_3^- was low, points lie equally above and below the horizontal 0 line. Variations in filtered load difference are in the range of 300 μmol/min and reflect corresponding fluctuations in GFR difference of ~5–10 ml/min.

Individual variability. The basal T − C pH difference varied among the 14 experiments (Fig. 6, *top left*, gray bars). In seven experiments, the T − C pH difference was >0 and the error bar did not cross the 0 line. In three more experiments, the mean exceeded 0 but the error bar crossed the 0 line.

Urine HCO_3^- excretion. Urine HCO_3^- excretion was higher in T than C kidneys (Fig. 6, *top middle*, gray bars), and the higher excretion reflected a higher FE (Table 3). NH_4Cl abolished the HCO_3^- differences (Fig. 6, *top middle*, black bars, Tables 2 and 3). Urine NH_4 excretions did not differ (Tables 2 and 3).

Origin of Increased Distal HCO_3^- Delivery

Increased delivery might arise from mTAL, cTAL, and possibly PT. To sort out these alternatives, we used additional measurements of solutes reabsorbed in these segments.

Urine flow rate. Urine flow was higher from T kidneys (Fig. 6, *top right*, gray bars; Tables 2 and 3), and time from SWL was significant in the ANOVA model (Table 3). NH_4Cl loading reduced but did not abolish the flow rate difference (Fig. 6, *top right*, black bars; Tables 2 and 3).

Na, Cl, and K excretions. All three mean basal T − C excretion differences exceeded 0 (Table 3; Fig. 6, *bottom*, gray bars) and were associated with increased FE (Table 3). Most experiments (Fig. 6) showed these effects. NH_4Cl loading abolished all three differences (Tables 2 and 3), although the NH_4Cl effect varied among experiments (Fig. 6, *bottom*, black bars).

Electrolyte free water clearance (CH_2O). Despite the flow rate difference (Table 3), basal T − C CH_2O did not differ from 0 (Table 3) because the higher urine flow rate was balanced by higher electrolyte (Na+K) excretion (Table 3). NH_4Cl reduced Na+K excretion more than urine flow rate so T − C CH_2O increased (Table 3). Since both kidneys receive identical blood vasopressin levels, why did urine volume of T not fall with electrolyte excretion? Urea is not the reason; after

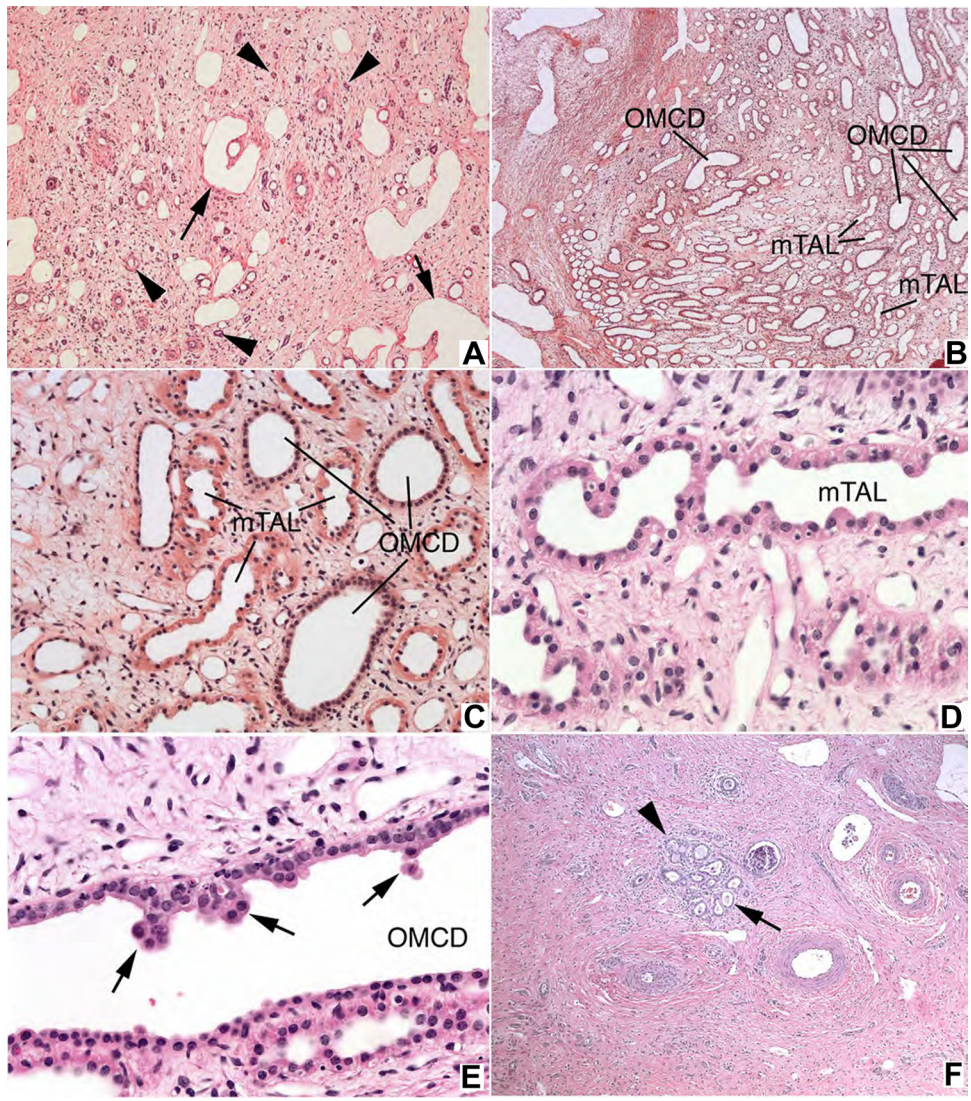

Fig. 3. Pattern of injury in the outer medulla of treated kidneys. The outer medulla of injured papillae were diffusely abnormal, ranging in severity from almost complete atrophy of all tubular segments (*A*, arrowheads) except for a few dilated medullary collecting ducts (arrows) to modest interstitial fibrosis associated with almost all medullary thick ascending limbs (mTAL) and outer medullary collecting ducts (OMCD; *A–E*) showing wavy irregularity and dilation. Lining cell epithelium of some OMCD was focally heaped up in a polypoid configuration (*E*, arrows). The S3 segments of proximal tubules (PT; *F*, arrows) adjacent to bands showed the variable loss of cell height and basement membrane thickening observed in cortical PT.

NH_4Cl loading, urea molarity was lower in T than C kidneys (Table 3). This suggests that water extraction by T kidneys is less efficient than in C kidneys and that the higher flow rate is not entirely due to higher Na+K excretion.

Ca and Mg. Excretion rates and FE for both were higher in T vs. C kidneys (Tables 2 and 3). NH_4Cl loading abolished the significance of the mean differences in excretion for both Ca and Mg, but FE Mg remained above 1 (Table 3). That FE Mg remained elevated despite acid loading speaks for an intrinsic abnormality of its transport as opposed to the effects of HCO_3^- delivery. The fact that FE Mg could remain high when differences in excretion were no longer high requires that filtered load fall; although statistically insignificant, T − C CCr did convert from positive to negative with acid loading (Tables 2 and 3).

Table 5. *Measurements of tubule hyperplasia in T and C kidneys*

	mTAL Diameter, μm		mTAL Cell No.		mCD Diameter, μm		mCD Cell No.	
Pig	C	T	C	T	C	T	C	T
910	40.86	62.94	4.94	8.98	61.74	116.22	13.26	20.64
916	42.30	65.46	5.38	9.24	60.06	110.94	13.70	20.60
921	46.38	68.70	4.84	8.78	64.14	129.72	13.74	24.22
983	36.30	59.40	4.70	8.72	58.80	135.06	12.36	21.30
1037	36.00	55.74	4.74	8.56	59.22	130.80	11.92	20.60
1038	34.32	57.90	4.62	6.66	56.22	117.66	11.42	19.12
1039	32.10	53.88	4.84	8.42	59.46	107.10	11.36	17.46
1040	30.90	48.84	5.00	8.26	55.74	98.46	11.00	17.52
Mean ± SE	37.40 ± 1.89	59.11 ± 2.29*	4.88 ± 0.08	8.45 ± 0.28*	59.42 ± 0.97	118.25 ± 4.52*	12.35 ± 0.39	20.18 ± 0.78*

mTAL, Medullary thick ascending limb; mCD, medullary collecting duct. *$P < 0.001$ vs. C, same group.

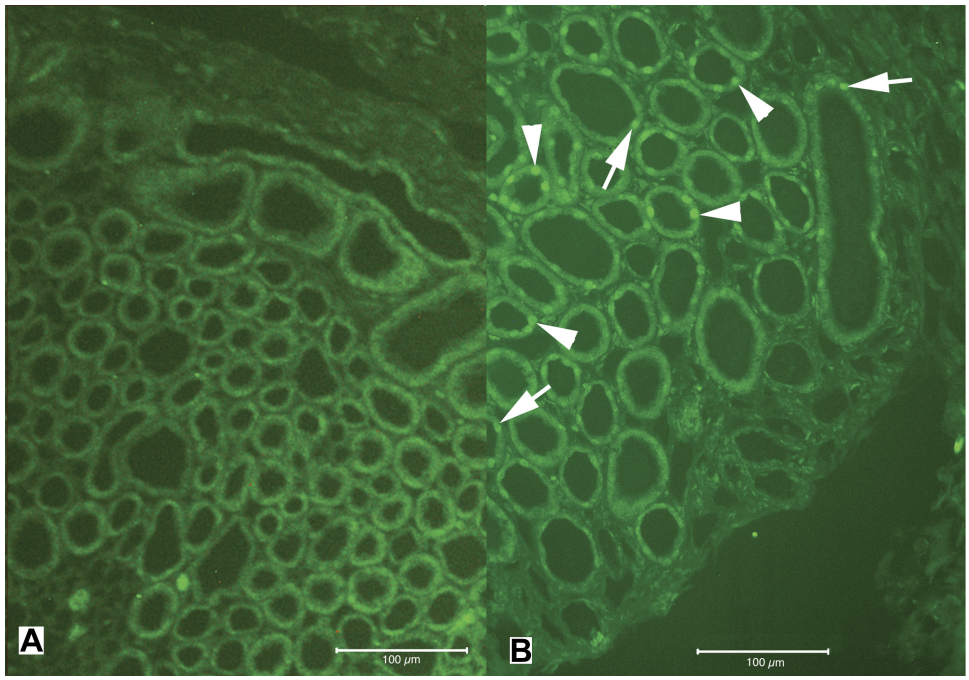

Fig. 4. Proliferating cells identified with Ki-67 antibody. Tissue sections of the outer medulla from the untreated (*A*) and treated (*B*) kidney from *pig 983* showed Ki-67-positive nuclei only in the mTAL (*B*, arrowheads) and OMCD (*B*, arrows) of the treated kidney.

Correlations Between (T − C) for Na, Ca, Cl, and Flow, and Renal Injury

In a full correlation matrix that included all the above measurements as well as basal and NH_4Cl excretion differences for K, Mg, HCO_3^- and FE ratios for creatinine, Na, Ca, Mg, Cl, HCO_3^-, and lithium, differences in urine pH, and degree of cortical and medullary injury, we found very highly significant correlations ($r = >0.9$, $P < 0.001$) only among Na, Ca, Cl, and flow (Fig. 7). That these correlations are so high, and remain as high as they do despite acid loading, speak for

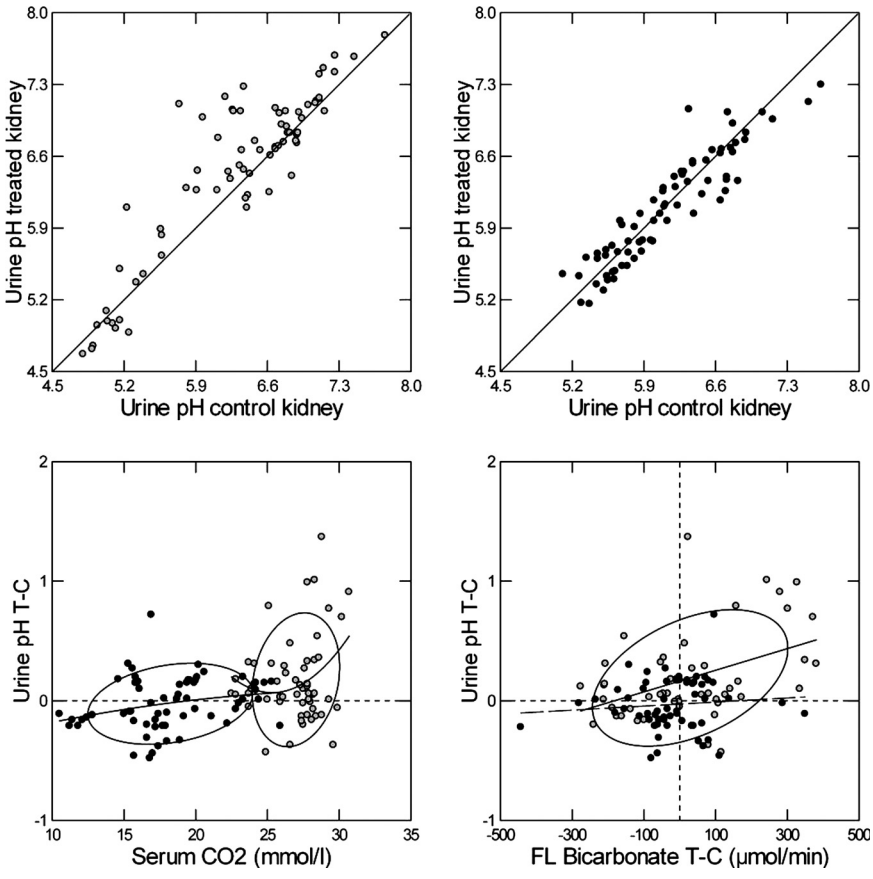

Fig. 5. Effects of shock wave lithotripsy (SWL) on urine pH. Urine pH of SWL-treated (T) kidneys (*top left*, *y*-axis) exceeded that of control (C) kidneys (*x*-axis) as shown by displacement of points above the diagonal line of identity. After induction of NH_4Cl acidosis (*top right*), the pH difference was abolished and points range above and below the line of identity. The T − C urine pH difference (*bottom left*, *y*-axis) varied significantly with serum HCO_3^- (*x*-axis) during NH_4Cl acidosis (black circles) but not under basal conditions (gray circles) even when points were fitted with a quadratic smoother (curving regression line). The T − C urine pH difference varied with the T − C bicarbonate-filtered load difference (*bottom right*, *x*-axis) in the basal (gray circles) but not NH_4Cl acidosis periods (black circles). However, the basal regression was not statistically significant. For visual clarity, 95% nonparametric ellipses of containment enclose the points of the *bottom* 2 panels.

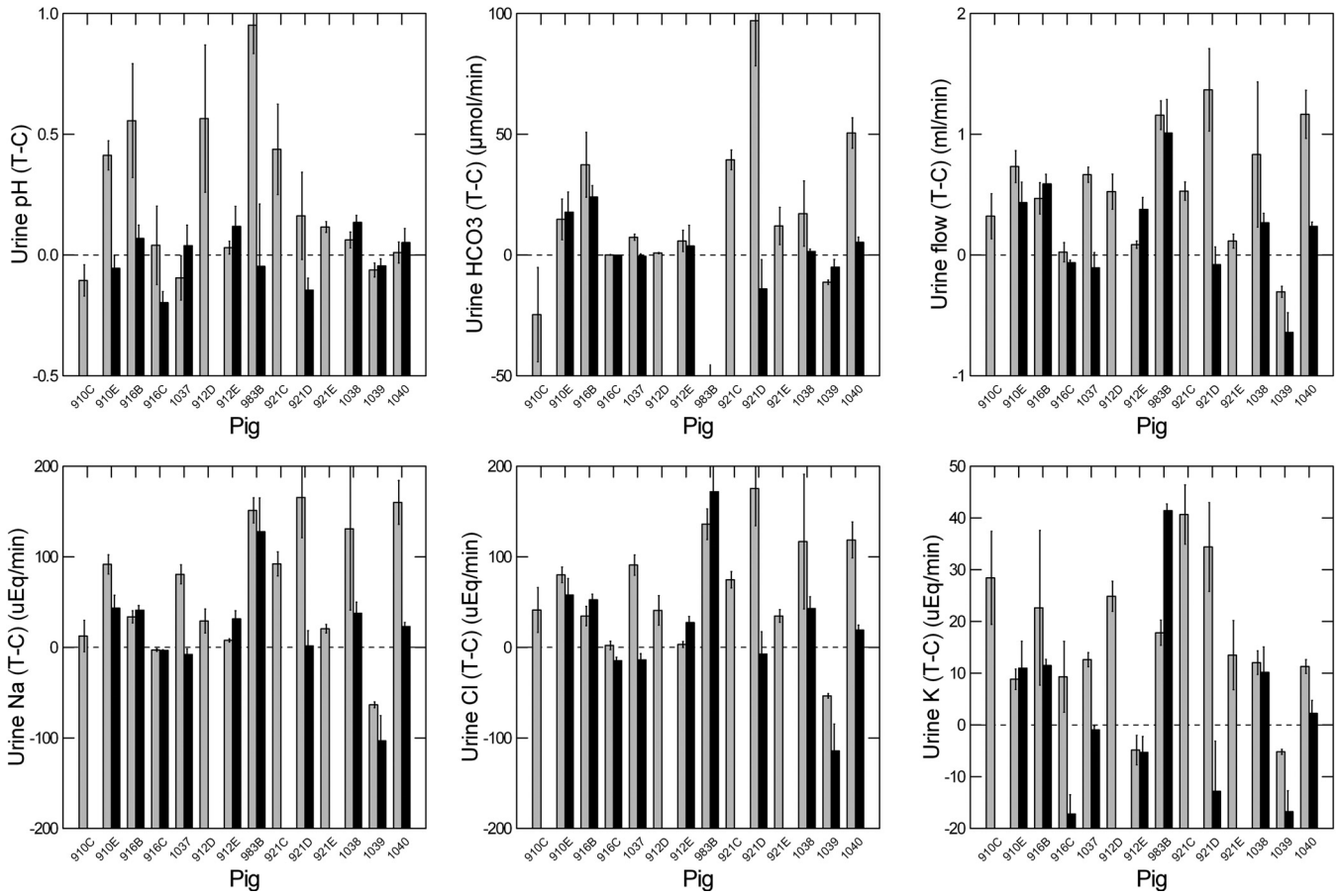

Fig. 6. T − C differences in pH, HCO_3^-, water, Na, Cl, and K excretion during individual experiments. In each panel, the experiments of Table 1 are shown along the *x*-axis. Gray bars represent the T − C mean basal difference for that experiment ± SE; black bars show NH_4Cl loading periods. The dashed horizontal lines represent a 0 difference.

an intrinsic defect of transport involving TAL. Histologically assessed renal injury did not correlate with any functional measurements.

PT-Related Solutes: Oxalate, PO_4, Urate, SO_4, and Lithium

Oxalate, PO_4, and urate. The oxalate T − C excretion difference exceeded 0, and the FE ratio exceeded 1 (Tables 2 and 3); the significance of both was abolished by NH_4Cl. Unfortunately, we did not obtain data in *experiments 1037–1040*. Phosphate handling did not differ between T and C kidneys except for a negative excretion difference (C>T) after NH_4Cl (Tables 2 and 3). Urate showed a similar pattern, with a negative T − C difference during NH_4Cl loading (Tables 2 and 3) and an FE ratio above 1 (Table 3). *Experiment 92* lacked phosphate measurements.

SO_4, lithium, and CCr. The SO_4 T − C excretion difference was highly significant (Tables 2 and 3). NH_4Cl abolished the T − C difference, but the FE ratio remained above 1 (Table 3). We could not obtain serum lithium values, but the serum value cancels out in the FE ratio, whose mean value was above 1 (Table 3). The T − C CCr difference was not significant (Tables 2 and 3), nor did the ratio of CCr values differ significantly from 1 (not shown).

DISCUSSION

SWL Raises Urine pH via Increased HCO_3^- Delivery

We began with the hypothesis that SWL can raise urine pH. In 14 experiments on 9 pigs, the mean pH of T kidneys exceeded that of the C kidneys by 0.18 units. By comparison, urine pH of IPSF exceeds that of ICSF by an equivalent amount, 0.25 pH units (29).

Increased HCO_3^- delivery to CD is at least partly responsible for the pH difference because NH_4Cl acidosis abolished it. Moreover, the urine pH difference varied with the level of blood total HCO_3^- content and with the difference in filtered HCO_3^- between T and C kidneys.

Local pH Differences May Exceed What We Observed

We measured bulk urinary pH from the ureter. If the magnitude of the HCO_3^- reabsorptive defect differs among nephrons, CD receiving fluid from the more badly damaged segments would have much higher lumen pH values and higher risk for CaP formation. In other words, the bulk urine is from all papillae and its pH, being an average, underestimates the potential extremes that may be produced by SWL. Since histological damage is focal, very high pH values in some CD is not an unreasonable hypothesis.

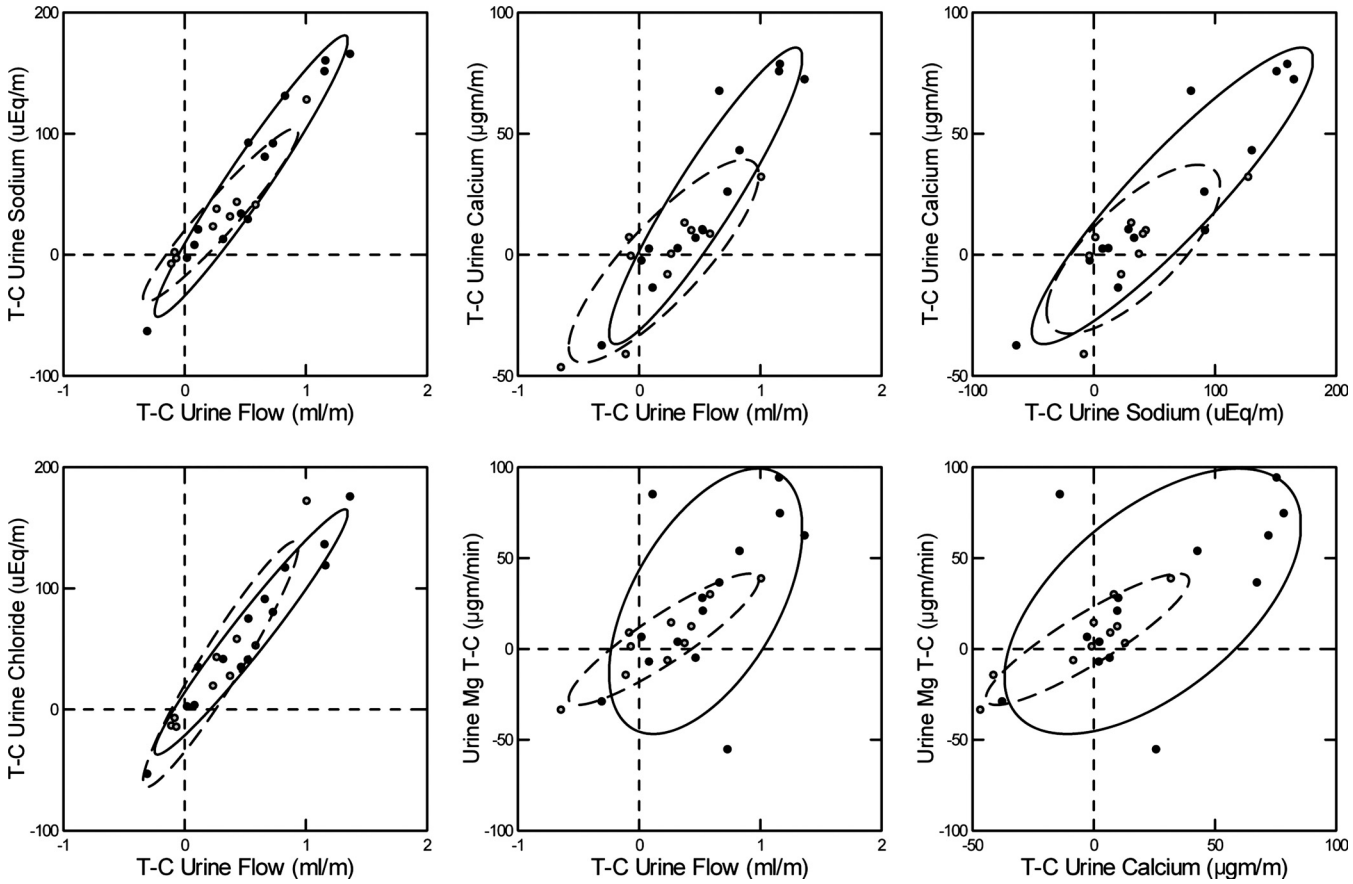

Fig. 7. Correlations between T − C differences in water, Cl, Ca, and Na excretions. Gray circles are basal periods, black circles are NH_4Cl acidosis periods. Non parametric confidence ellipses are calculated to include 68% of points. All regressions are highly significant ($r > 0.9$, $P < 0.001$).

TAL Injury May Increase HCO_3^- Delivery to CD

T kidneys excreted more Na, K, HCO_3^-, water, Ca, Mg, and Cl than C kidneys. A single nephron site that could produce losses of all of these is TAL (15). TAL reabsorbs filtered HCO_3^- via NHE3 (2), so a TAL defect could deliver excessive amounts of HCO_3^- to CD and raise tubule fluid pH.

In TAL, Na and Cl are reabsorbed via the Na-K-2Cl cotransporter (NKCC2). Potassium is reabsorbed and recycled via the renal outer medullary K channel (ROMK) (15). The dilute effluent enters CCD, wherein water is reabsorbed to achieve isotonicity to plasma. When TAL reabsorbs less NaCl, less water can be reabsorbed, increasing final urine volume. Ca and Mg are reabsorbed by TAL mainly electrogenically via the lumen positive potential generated by the activity of NKCC2 and coupled K recycling via ROMK. In our experiments, urine excretion differences (T − C) for Na, Cl, Ca, and urine flow were intensely correlated, a fact compatible with reduced TAL reabsorption. Altogether, if any one segment were to be singled out as a candidate for further study, it would be TAL.

Transport properties of cTAL and mTAL are broadly similar, and we found histopathological changes in both. But changes were far more marked in mTAL, and the vascular anatomy of mTAL is more vulnerable to SWL than that of cTAL (25). For these reasons, we believe it was an mTAL defect that produced the bulk of the electrolyte abnormalities in our pigs.

PT Injury May Contribute to Increased CD HCO_3^- Delivery

The high urine SO_4 and oxalate losses we observed, as well as elevated FE ratios for lithium (T/C), are likely due to PT injury. Oxalate is secreted and reabsorbed in PT via SLC26a6 and SLC26a1 (33). Because sulfate is reabsorbed via NaSi and SLC26a1, and recycled on multiple PT transporters (22), the SO_4 losses we observed are best explained by a PT injury. The increase in the T/C FE lithium ratio is evidence for reduced NaCl and water reabsorption by PT in the T kidneys (37). Taken together, these three abnormalities are best explained by PT injury reducing PT solute reabsorption.

We do not have any explanation for the slight abnormalities of phosphate and urate excretions by T kidneys: reduced excretion for both in the basal experiments, and an increased FE ratio for urate with NH_4Cl. Defects in PT transport do not usually affect all transport systems equally, so some heterogeneity is not surprising.

Integration of Histopathology and Pathophysiology

mTAL and mCD were far more injured than cTAL and CCD. Their elongation and wavy appearances, as well as direct measurement of nuclear Ki-67 protein, which is present during all active phases of the cell cycles (G_1, S, G_2, and mitosis), their large increases in the number of epithelial cells, and their increased tubule diameters all seem consequences of injury

followed by cell proliferation and attempted repair. Active cell proliferation was ongoing at the time the tissue was harvested, meaning that it was present at the time of our physiological studies.

It is generally known that epithelial cells lose their polarity and therefore their capacity for normal vectoral transport as they proliferate as part of the repair process (34). We therefore propose the following:

1) SWL injured mTAL cells both directly through cavitation in nearby blood pools after rupture of capillary beds, and indirectly through ischemia from disruption of inner medullary ascending vasa recta which normally provide blood flow to mTAL (25).

2) After injury, mTAL cells began the process of repair via proliferation.

3) That process was not complete even as far as 70 days after SWL.

4) Reduced cell polarity, an established feature of proliferation during repair, reduced mTAL transport and led to high HCO_3^- delivery to CD, which raised urine pH, and to abnormal losses of Na, K, Cl, Ca, Mg, and water.

5) OMCD epithelial cells also were proliferating at the time the tissues were harvested; we presume their transport functions would also have been impaired, including those of the OMCD intercalated cells which express the V-ATPase. We could not test this point experimentally.

6) OMCD and IMCD injury, as well as loss of normal papillary architecture, account for that component of higher urine volume of SWL-treated kidneys which is not due to increased solute excretion.

Injury Mediators

The mechanisms fostering proliferation of mTAL and OMCD cells after injury probably included oxidative stress. In pigs, SWL regularly increases hemoxygenase type 1 (HO-1), which is a mediator of oxidative stress. Although we did not measure HO-1 here, we have in acute SWL pig studies (3) and found it high.

Mechanism for High K Excretion

The high urine K excretion of T vs. C kidneys probably reflects high delivery of Na-HCO_3 to CD and need not be ascribed to CCD or OMCD injury. Na reabsorption via ENaC is electrogenic (12). If the ratio of HCO_3^- to Cl were increased by high HCO_3^- delivery, the HCO_3^- being incompletely reabsorbed would increase the transmembrane potential difference from ENaC, thereby increasing intratubular fluid K concentration (19). The higher water delivery from mTAL would increase K excretion, which is flow dependent (19). As would be expected, the T − C K excretion difference disappeared with acidosis.

PT Contributions to SWL pH Elevation

The bulk of cortical PT was normal. Abnormalities were restricted to regions immediately adjacent to scars, which were themselves sparse. In the outer medulla, PT seemed mainly normal in appearance. Even so, SO_4 and lithium handling were abnormal. Perhaps the small fraction of morphologically abnormal PT contributed to these functional changes. More likely, functional alterations were present in otherwise normal appearing cells. We have no way of estimating the magnitude of excess PT HCO_3^- delivery in T kidneys.

The Abnormalities We Have Observed Would Not Be Evident in Patients

Although SWL is a common procedure, clinicians could never observe these disorders of fluid and electrolytes. Even if one kidney were so extensively shocked as in our pigs, the mixed bladder urine from the two kidneys would be normal. Given only one kidney, systemic adaptation to brief excesses of NaCl and water loss would reduce such losses, and moreover there could be no meaningful controls for comparison. Only humans with bilateral ureteral catheters in place who had one kidney extensively shocked could possibly manifest what we observed here. In the calyceal environment of a shocked kidney, high pH and electrolyte losses could be common, and be promoting CaP stones, yet go undetected.

Our Experiments Do Not Permit Assessment of CaP Stone-Forming Potential

Our pigs were studied under anesthesia and fasting. We could not measure urine citrate because levels were below detection by our methods. If the pigs were studied while awake and eating, and if the pH difference were persistent, which is likely, and if the normal conditions of pig urine can permit CaP SS, then the higher pH would per force raise CaP SS and foster CaP stones. Our design and intent did not include the necessary measurements to explore these matters. For all of these reasons, we cannot quantify the effects of the 0.18-unit increase in urine pH on urine CaP SS in our animals. However, this experiment provides a rationale to support the clinical observations that SWL is an apparent risk factor for CaP stones, and therefore supports the need for additional clinical research.

Our Experiments Are Relevant to Clinical SWL

We recognize that the total energy delivered to the kidneys of these pigs exceeds by fourfold that encountered by human kidneys in the course of clinical SWL therapy; however, the high-energy delivery was used in such a way as to minimize this problem. To use bulk urine from a whole kidney, we had to provide SWL to the whole kidney. To do this, we calculated the width of the shock wave path and found that, given the size of the kidneys, the energy would have to be provided in four zones. For each zone, we applied the standard clinical dose of 2,000 shock waves. Although the total energy to the kidney was 8,000 shock waves, no one zone received >2,000 shocks. Therefore, these results are broadly applicable to human SWL treatment.

Summary

SWL produces widespread tubule cell injury easily observed histopathologically that leads to functional disturbances across a wide range of electrolyte metabolism, including higher than control urine pH. Effects of SWL were detected up to 70 days after one treatment. Given a normal contralateral kidney, these effects would be obscured by the actions of the normal kidney. Similarly, the normal kidney, which could in fact support the entire organism, can easily compensate for such losses by corresponding increases in reabsorption so that fluid and elec-

trolyte balance can remain normal. Clinically, the disorder we have observed would go unnoticed and would be of no interest except for the potential of higher pH to engender CaP stones.

GRANTS

This work was funded by National Institutes of Health Grants PO1 DK56788 and PO1 DK43881.

DISCLOSURES

J. Lingeman has a financial interest in Midwest Mobile Lithotripsy and Midstate Mobile Lithotripsy.

AUTHOR CONTRIBUTIONS

Author contributions: A.P.E., F.L.C., B.A.C., R.K.H., J.E.L., and E.M.W. provided conception and design of research; A.P.E., F.L.C., B.A.C., R.K.H., J.E.L., and E.M.W. performed experiments; A.P.E., F.L.C., B.A.C., R.K.H., and E.M.W. analyzed data; A.P.E., F.L.C., B.A.C., R.K.H., and E.M.W. interpreted results of experiments; A.P.E., F.L.C., and E.M.W. prepared figures; A.P.E., F.L.C., B.A.C., R.K.H., J.E.L., and E.M.W. drafted manuscript; A.P.E., F.L.C., B.A.C., R.K.H., J.E.L., and E.M.W. edited and revised manuscript; A.P.E., F.L.C., B.A.C., R.K.H., J.E.L., and E.M.W. approved final version of manuscript.

REFERENCES

1. **Bhojani N, Paonessa JE, Worcester EM, van AP, Coe FL, Lingeman JE.** The majority of calcium phosphate stone formers without systemic disease have nephrocalcinosis. *J Urol* 189: e924–e925, 2013.
2. **Capasso G, Unwin R, Rizzo M, Pica A, Giebisch G.** Bicarbonate transport along the loop of Henle: molecular mechanisms and regulation. *J Nephrol* 15, *Suppl* 5: S88–S96, 2002.
3. **Clark DL, Connors BA, Evan AP, Willis LR, Handa RK, Gao S.** Localization of renal oxidative stress and inflammatory response after lithotripsy. *BJU Int* 103: 1562–1568, 2009.
4. **Daudon M, Donsimoni RHC, Fellahi S, Le Moel G, Paris M, Troupel S, Lacour B.** Sex and age-related composition of 10617 calculi analyzed by infrared spectropscopy. *Urol Res* 23: 326, 1995.
5. **Drach GW, Dretler S, Fair W, Finlayson B, Gillenwater J, Griffith D, Lingeman J, Newman D.** Report of the United States cooperative study of extracorporeal shock wave lithotripsy. *J Urol* 135: 1127–1133, 1986.
6. **Dretler SP.** Stone fragility—a new therapeutic distinction. *J Urol* 139: 1124–1127, 1988.
7. **Evan AP, McAteer JA.** Q-effects of shock wave lithotripsy. In: *Kidney Stones: Medical and Surgical Management*, edited by Coe FL, Pak CYC, and Preminger GM. New York: Raven, 1996, p. 549–570.
8. **Evan AP, Lingeman JE, Coe FL, Parks JH, Bledsoe SB, Shao Y, Sommer AJ, Paterson RF, Kuo RL, Grynpas M.** Randall's plaque of patients with nephrolithiasis begins in basement membranes of thin loops of Henle. *J Clin Invest* 111: 607–616, 2003.
9. **Evan AP, Lingeman JE, Coe FL, Shao Y, Parks JH, Bledsoe SB, Phillips CL, Bonsib S, Worcester EM, Sommer AJ, Kim SC, Tinmouth WW, Grynpas M.** Crystal-associated nephropathy in patients with brushite nephrolithiasis. *Kidney Int* 67: 576–591, 2005.
10. **Evan AP, Lingeman JE, Worcester EM, Sommer AJ, Phillips CL, Williams JC, Coe FL.** Contrasting histopathology and crystal deposits in kidneys of idiopathic stone formers who produce hydroxy apatite, brushite, or calcium oxalate stones. *Anat Rec (Hoboken)* 297: 731–748, 2014.
11. **Evan AP, Willis LR, Lingeman JE, McAteer JA.** Renal trauma and the risk of long-term complications in shock wave lithotripsy. *Nephron* 78: 1–8, 1998.
12. **Kashlan OB, Kleyman TR.** Epithelial Na^+ channel regulation by cytoplasmic and extracellular factors. *Exp Cell Res* 318: 1011–1019, 2012.
13. **Klee LW, Brito CG, Lingeman JE.** The clinical implications of brushite calculi. *J Urol* 145: 715–718, 1991.
14. **Krambeck AE, Handa SE, Evan AP, Lingeman JE.** Profile of the brushite stone former. *J Urol* 184: 1367–1371, 2010.
15. **Kriz W, Kaissling B.** Structural organization of the mammalian kidney. In: *Seldin and Giebisch's The Kidney: Physiology and Pathophysiology*, edited by Alpern RJ, Moe OW, and Caplan M. Amsterdam: Elsevier, 2013, p. 595–691.
16. **Kriz W.** Structural organization of the renal medulla: comparative and functional aspects. *Am J Physiol Regul Integr Comp Physiol* 241: R3–R16, 1981.
17. **Lingeman JE, Matlaga BR, Evan AP.** Surgical management of upper urinary tract calculi. In: *Campbell-Walsh Urology*, edited by Wein AJ, Kavoussi LR, Novick AC, Partin AW, and Peters CA. Philadelphia: Saunders, 2007, p. 1431–1507.
18. **Lingeman JE, Newman D, Mertz JH, Mosbaugh PG, Steele RE, Kahnoski RJ, Coury TA, Woods JR.** Extracorporeal shock wave lithotripsy: the Methodist Hospital of Indiana experience. *J Urol* 135: 1134–1137, 1986.
19. **Malnic G, Geibisch G, Muto S, Wang W, Bailey MA, Satlin LM.** Regulation of potassium excretion. In: *Seldin and Giebisch's The Kidney: Physiology and Pathophysiology*, edited by Alpern RJ, Moe OW, and Caplan M. Amsterdam: Elsevier, 2013, p. 1659–1715.
20. **Mandel NS, Mandel GS.** Urinary tract stone disease in the United States veteran population. II. Geographical analysis of variations in composition. *J Urol* 142: 1516–1521, 1989.
21. **Mandel NS, Mandel I, Fryjoff K, Rejniak T, Mandel GS.** Conversion of calcium oxalate to calcium phosphate with recurrent stone episodes. *J Urol* 169: 2026–2029, 2003.
22. **Markovich D.** Physiological roles of renal anion transporters NaS1 and Sat1. *Am J Physiol Renal Physiol* 300: F1267–F1270, 2011.
23. **Matlaga BR, McAteer JA, Connors BA, Handa RK, Evan AP, Williams JC, Lingeman JE, Willis LR.** Potential for cavitation-mediated tissue damage in shockwave lithotripsy. *J Endourol* 22: 121–126, 2008.
24. **Maurice-Estepa L, Levillain P, Lacour B, Daudon M.** Crystalline phase differentiation in urinary calcium phosphate and magnesium phosphate calculi. *Scand J Urol Nephrol* 88: 299–305, 1999.
25. **McAteer JA, Evan AP.** The acute and long-term adverse effects of shock wave lithotripsy. *Semin Nephrol* 28: 200–213, 2008.
26. **Parks JH, Coe FL, Evan AP, Worcester EM.** Clinical and laboratory characteristics of calcium stone-formers with and without primary hyperparathyroidism. *BJU Int* 103: 670–678, 2009.
27. **Parks JH, Coe FL, Evan AP, Worcester EM.** Urine pH in renal calcium stone formers who do and do not increase stone phosphate content with time. *Nephrol Dial Transplant* 24: 130–136, 2009.
28. **Parks JH, Coward WM, Coe FL.** Correspondence between stone composition and urine supersaturation in nephrolithiasis. *Kidney Int* 51: 894–900, 1997.
29. **Parks JH, Worcester EM, Coe FL, Evan AP, Lingeman JE.** Clinical implications of abundant calcium phosphate in routinely analyzed kidney stones. *Kidney Int* 66: 777–785, 2004.
30. **Scholzen T, Gerdes J.** The Ki-67 protein: from the known and the unknown. *J Cell Physiol* 182: 311–322, 2000.
31. **Shao Y, Connors BA, Evan AP, Willis LR, Lifshitz DA, Lingeman JE.** Morphological changes induced in the pig kidney by extracorporeal shock wave lithotripsy: nephron injury. *Anat Rec A Discov Mol Cell Evol Biol* 275: 979–989, 2003.
33. **Soleimani M.** SLC26 Cl^-/HCO_3^- exchangers in the kidney: roles in health and disease. *Kidney Int* 84: 657–666, 2013.
34. **Wagner MC, Molitoris BA.** Renal epithelial polarity in health and disease. *Pediatr Nephrol* 13: 163–170, 1999.
35. **Willis LR, Evan AP, Connors BA, Blomgren P, Fineberg NS, Lingeman JE.** Relationship between kidney size, renal injury, and renal impairment induced by shock wave lithotripsy. *J Am Soc Nephrol* 10: 1753–1762, 1999.
36. **Willis LR, Evan AP, Connors BA, Reed G, Fineberg NS, Lingeman JA.** Effects of extracorporeal shock wave lithotripsy to one kidney on bilateral glomerular filtration rate and PAH clearance in minipigs. *J Urol* 156: 1502–1506, 1996.
37. **Worcester EM, Coe FL, Evan AP, Bergsland KJ, Parks JH, Willis LR, Clark DL, Gillen DL.** Evidence for increased postprandial distal nephron calcium delivery in hypercalciuric stone-forming patients. *Am J Physiol Renal Physiol* 295: F1286–F1294, 2008.
38. **Yang C, Stingo FC, Ahn KW, Liu P, Vannucci M, Laud PW, Skelton M, O'Connor P, Kurth T, Ryan RP, Moreno C, Tsaih SW, Patone G, Hummel O, Jacob HJ, Liang M, Cowley AW Jr.** Increased proliferative cells in the medullary thick ascending limb of the loop of Henle in the Dahl salt-sensitive rat. *Hypertension* 61: 208–215, 2013.